3D Acquisition Algorithmic Pipeline

David Gu

Computer Science Department
Stony Brook University

gu@cs.stonybrook.edu

August 4, 2022

Phase Shifting Structured Light

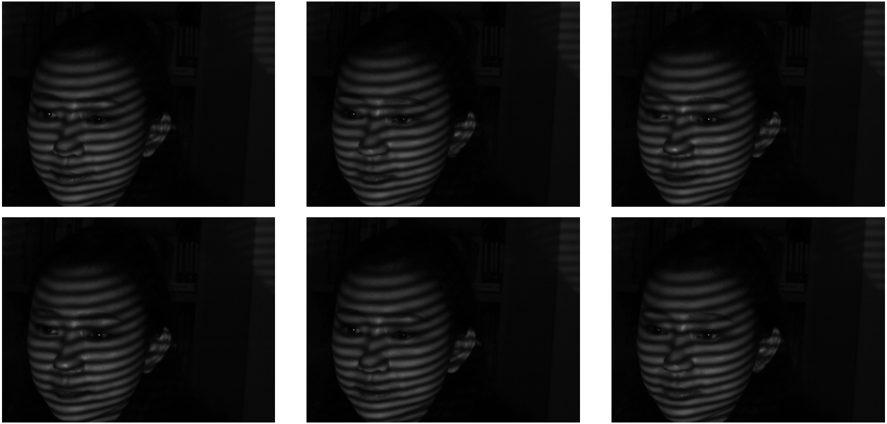

Figure: double wavelength phase shifting fringe images.

Phase Shifting Structured Light

Figure: Ambient, modulation, relative phase.

Phase Shifting Structured Light

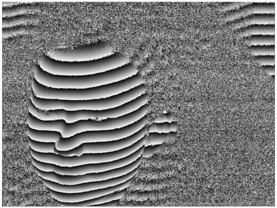

relative phase λ_1

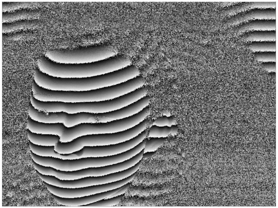

relative phase λ_2

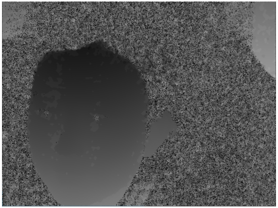

absolute phase

Figure: Phase Unwrapping

Phase Shifting Structured Light

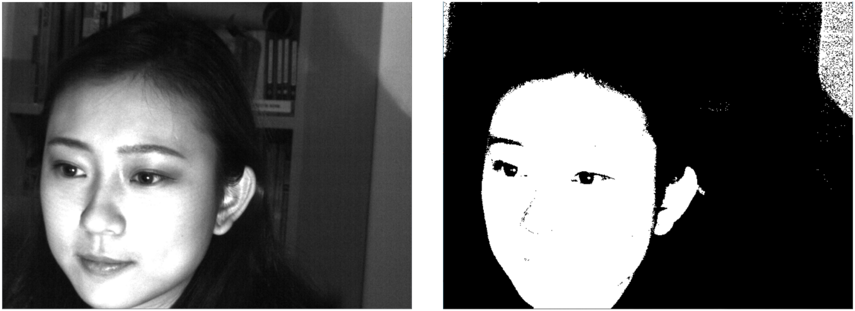

Figure: Image segmentation.

Phase Shifting Structured Light

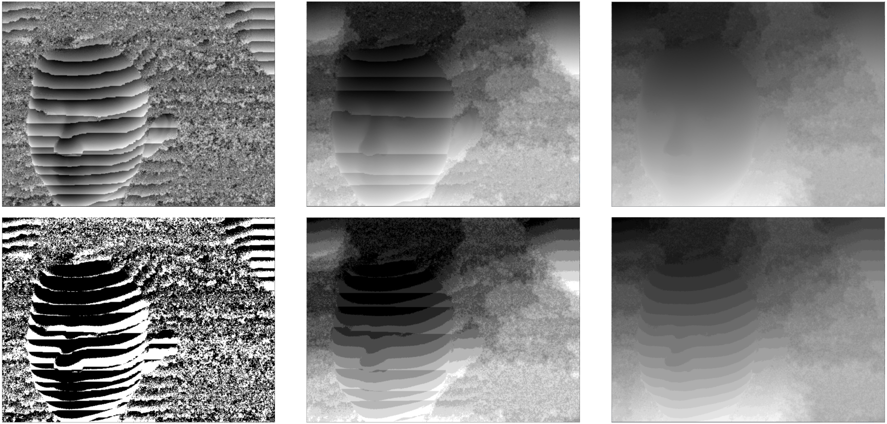

Figure: Unwrapped phases and wrap counts.

Phase Shifting Structured Light

Figure: Color texture image.

Phase Shifting Structured Light

Figure: Reconstructed 3D point clouds.

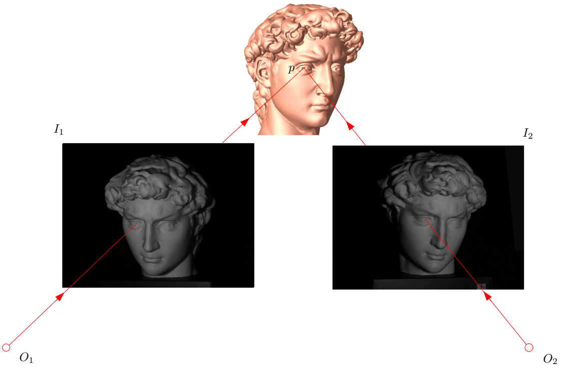

Triangulation principle

Reconstructed point cloud

Figure: Stereo-vision triangulation principle for reconstruction. The left and right camera images are I_1 and I_2, the optical centers are O_1 and O_2 respectively.

Stereo-Vision

Figure: Experimental setup.

Stereo-Vision

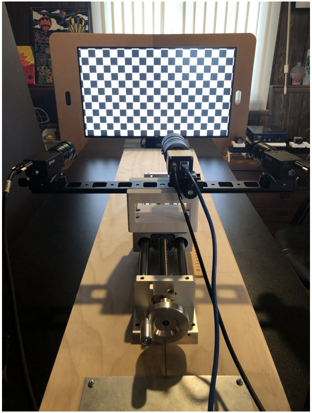

calibration mode.

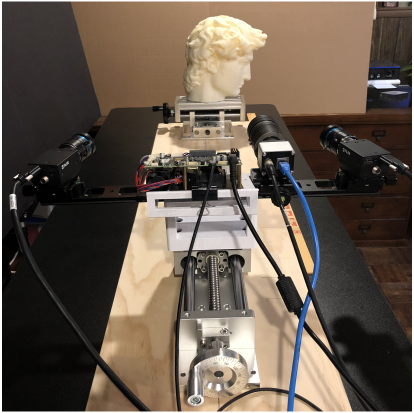

capture mode.

Figure: The calibration mode and the capture mode for the stereo-camera system.

Stereo-Vision

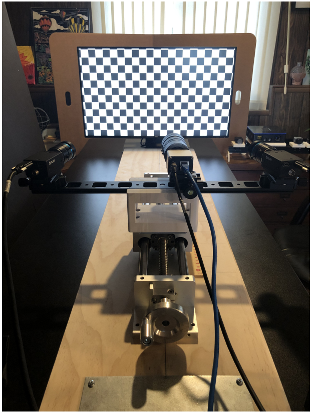

calibration mode.

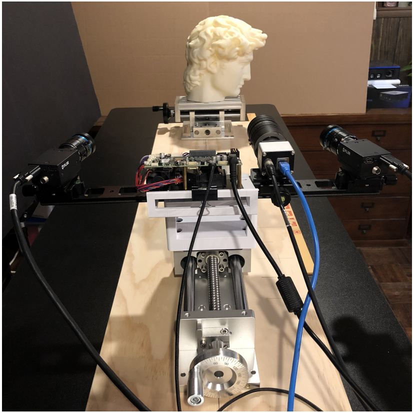

capture mode.

Figure: The calibration mode and the capture mode for the stereo-camera system.

Stereo-Vision

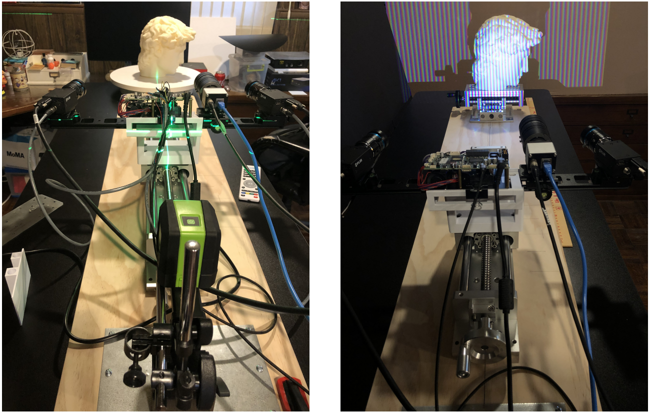

Figure: Structured light with the stereo-vision system.

Camera Calibration

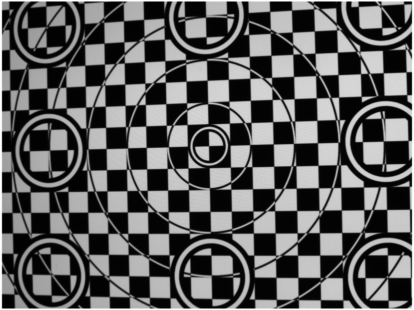

(a) physical camera image

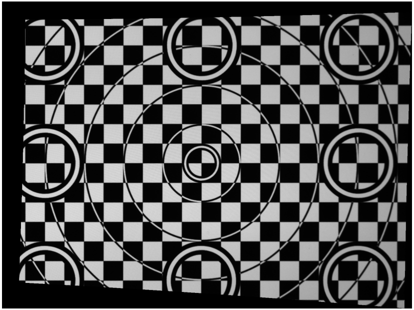

(b) virtual camera image

Figure: Comparision between the real image captured by our physical camera and the the image of our virtual camera at $Z_w = 0$. On the physical image, some circles are distorted to ellipses, on the virtual image, they are corrected to circles.

Epipolar Rectification

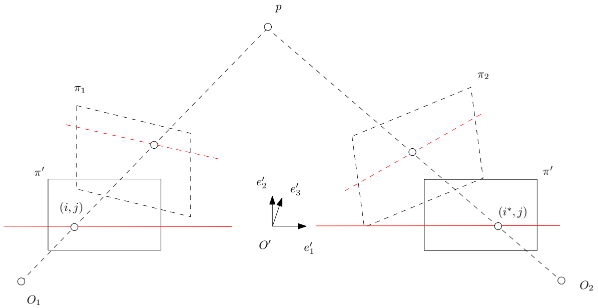

Figure: Epipolar rectification.

Epipolar Rectification

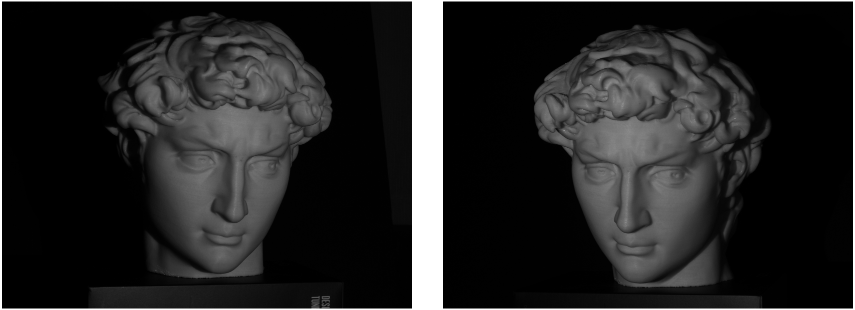

Figure: Raw images before epipolar rectification.

Epipolar Rectification

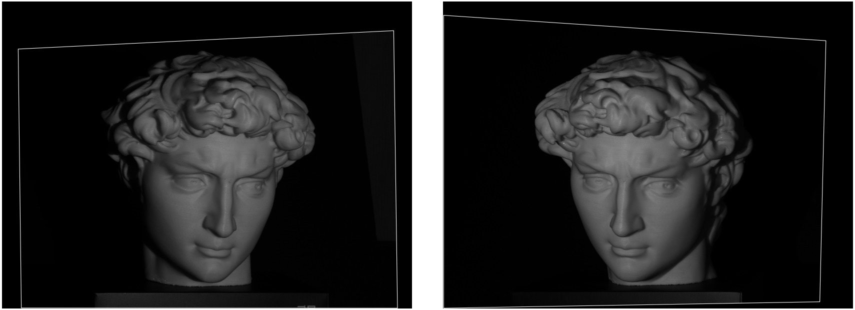

Figure: Epipolar rectification results.

Stereo-vision with Structured Light

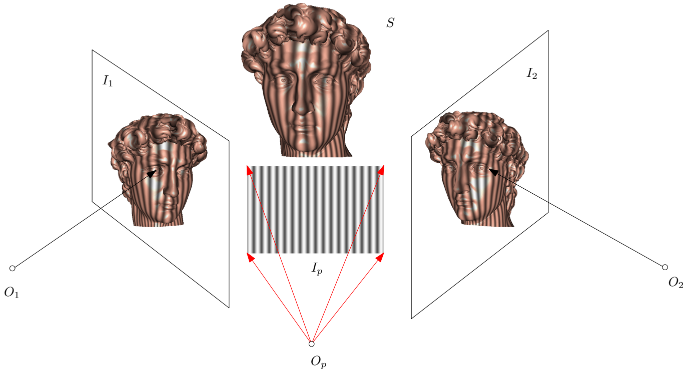

Figure: The fringe pattern for the digital projector or the LCD display. The left and right camera optical centers and image planes are (O_1, I_1) and (O_2, I_2) respectively. The projector optical center and image plane are (O_p, I_p).

Segmentation

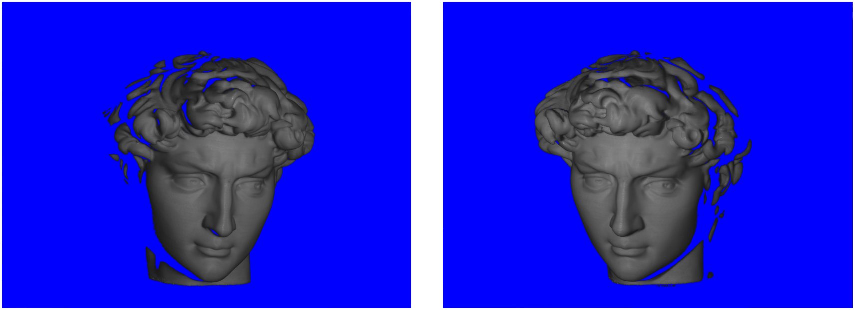

Figure: Segmentation results.

Disparity Map

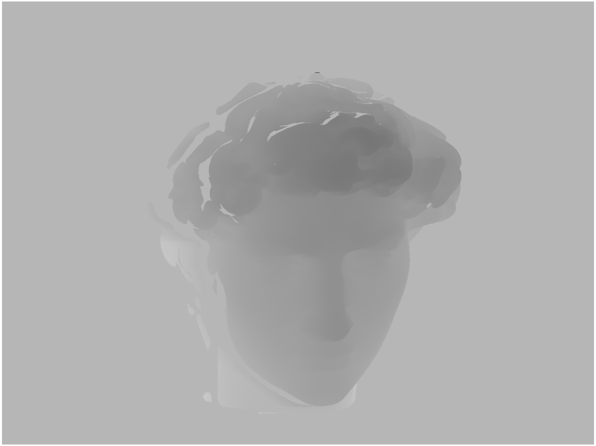

Figure: Disparity Map.

Point Cloud

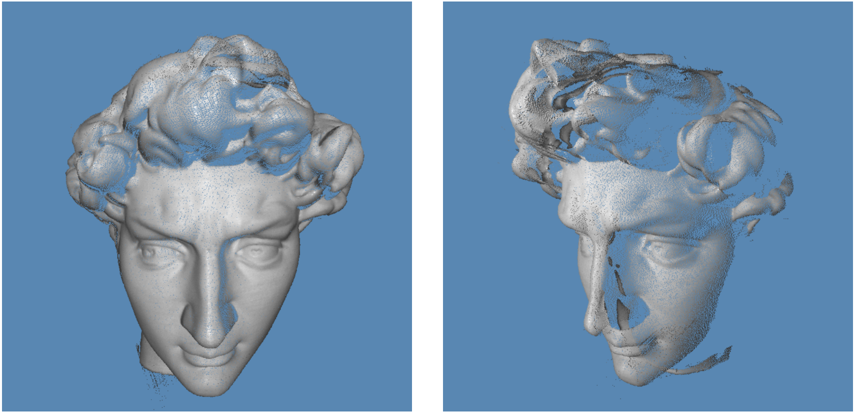

Figure: Reconstructed 3D point cloud, captured from different view angles.

Point Clouds

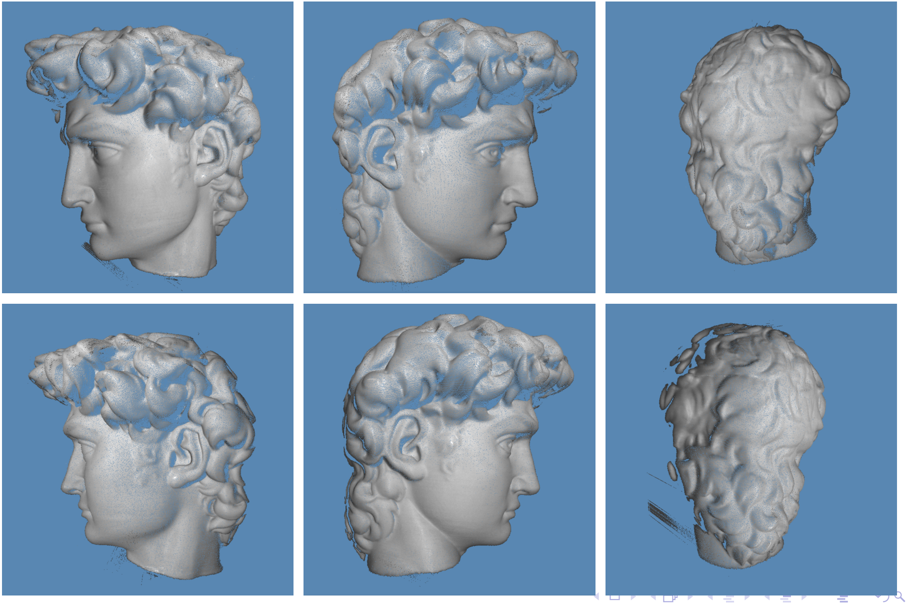

Point Cloud Fusion and Mesh Reconstruction

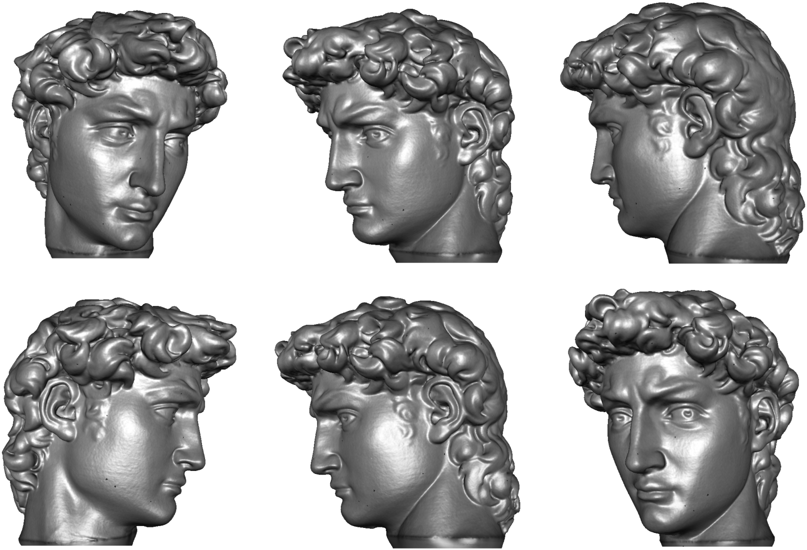

Figure: Reconstructed 3D Surface from scanned point clouds.

3D Printed Model

Figure: 3D printed model and the original object.

Point Cloud Fusion

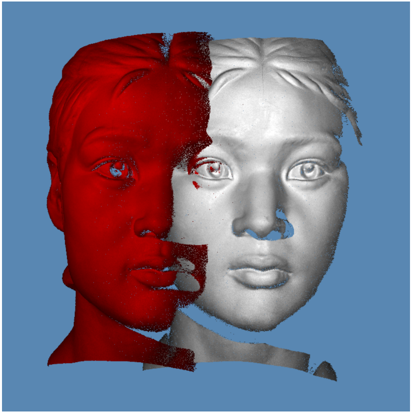

(a). before fusion

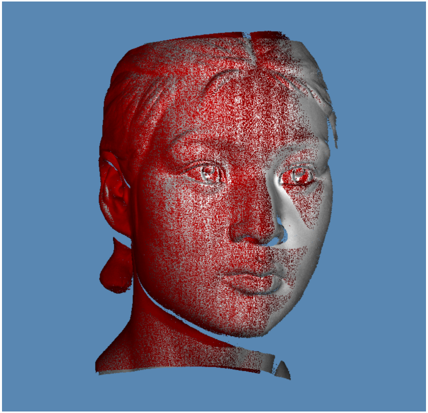

(b). after fusion

Figure: Point cloud fusion.

Normal Estimation

(a). merged point clouds

(b). with estimated normal

Figure: Normal estimation.

Point Cloud Fusion

One of the fundamental problems in SLAM (Simultaneous localization and mapping) is to fuse point clouds with global consistency.

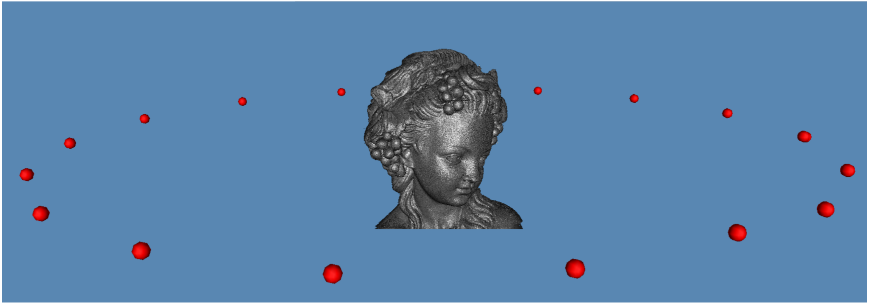

Figure: point cloud fusion with global consistency.

Loop Close Problem

Definition (View Graph)

The view graph $G = (V, E)$ is a graph, where each node represents a point cloud, each edge represents two overlapping point clouds.

Problem (Loop Close)

Given a view graph $G = (V, E)$, for each oriented edge $[n_i, n_j]$, find a rigid motion (a rotation and translation) from n_i to n_j, T_{ij}, such that, for each loop γ with ordered nodes $n_0, n_1, \cdots, n_{k-1}$, the composition

$$T_{k-1,0} \circ T_{k-2,k-1} \circ \cdots \circ T_{1,2} \circ T_{0,1} = Id.$$

Point Cloud Normal Estimation

Figure: Normal estimation for merged point clouds.

Poisson Mesh Reconstruction

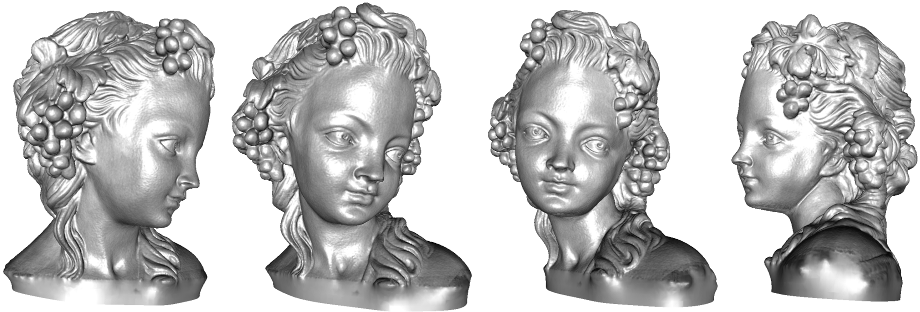

Figure: Poisson mesh reconstruction.

Poisson Mesh Reconstruction

Figure: 3D printed model and the original sculpture.

Surface Mesh Generation - Key Idea

Key Idea

Find a special diffeomorphism $\varphi : (S, \mathbf{g}) \to \Omega$ maps the 3D surface onto a planar domain, and converts the 3D meshing problem to a 2D planar meshing problem.

Figure: 3D meshing problems are converted to 2D meshing ones.

Special Mappings

- Angle preserving maps: keep the minimal angles;
- Area preserving maps: keep the grading;
- impossible to keep both, otherwise it is isometric.

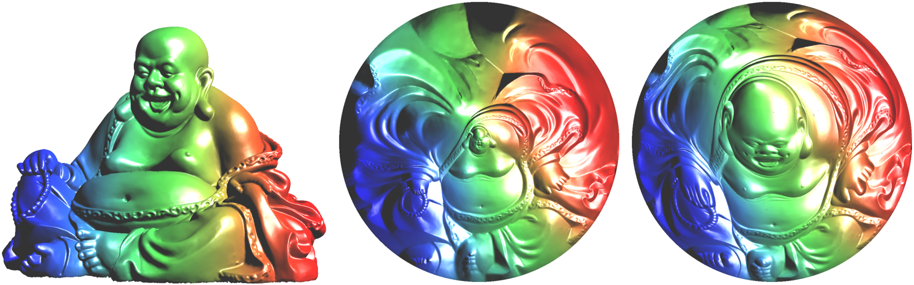

Figure: Conformal and optimal transport maps.

Surface Remesh

Figure: Conformal mapping by discrete surface Ricci flow.

Surface Remesh

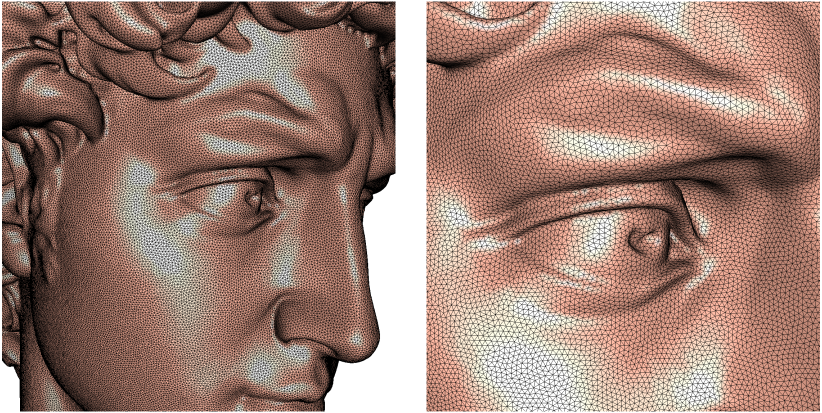

Figure: Conformal mapping by discrete surface Ricci flow.

Surface Remesh

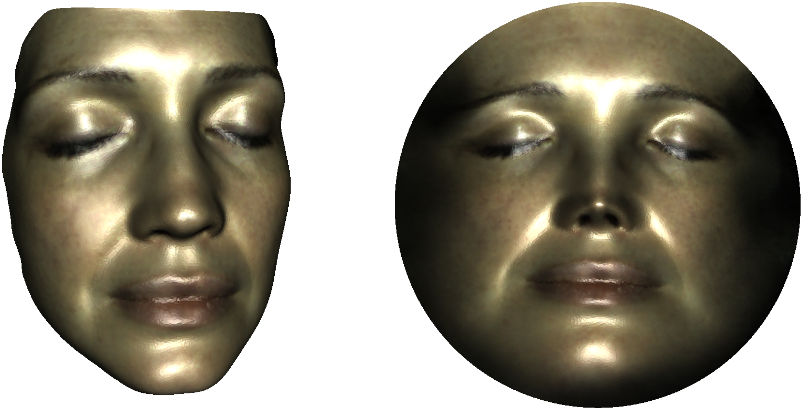

Figure: Conformal mapping by discrete surface Ricci flow.

Surface Remesh

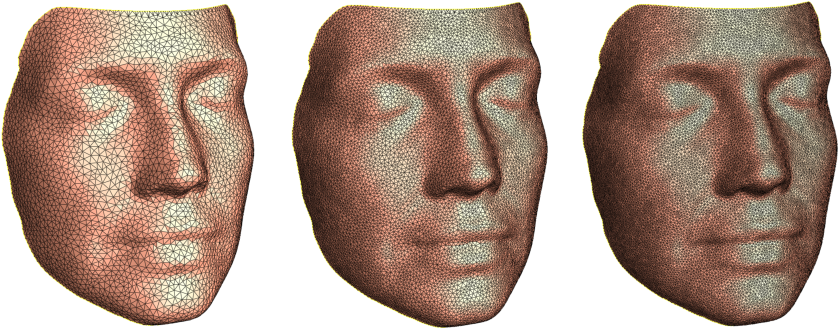

Figure: Multi-resolution Remeshing results.

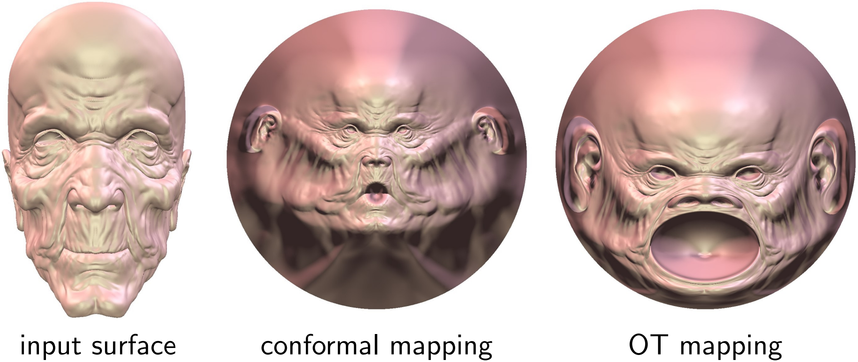

Figure: Conformal and optimal transport mappings.

Surface Multiresolution Compression

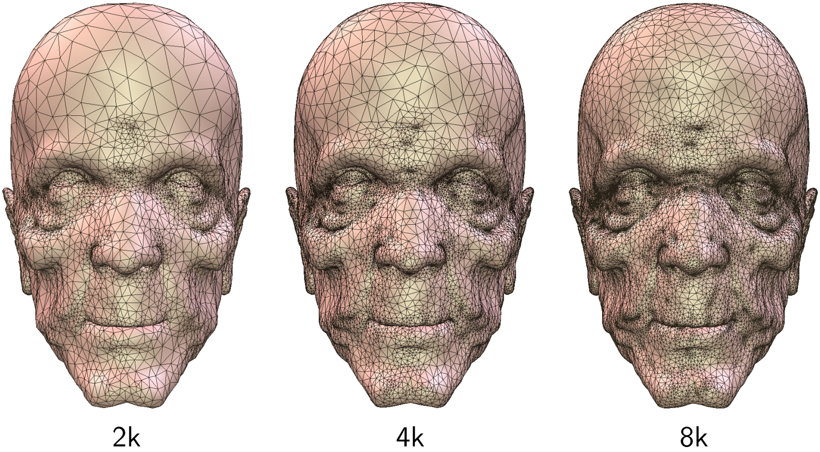

Figure: Multi-resolution Remeshing results.

Surface Multiresolution Compression

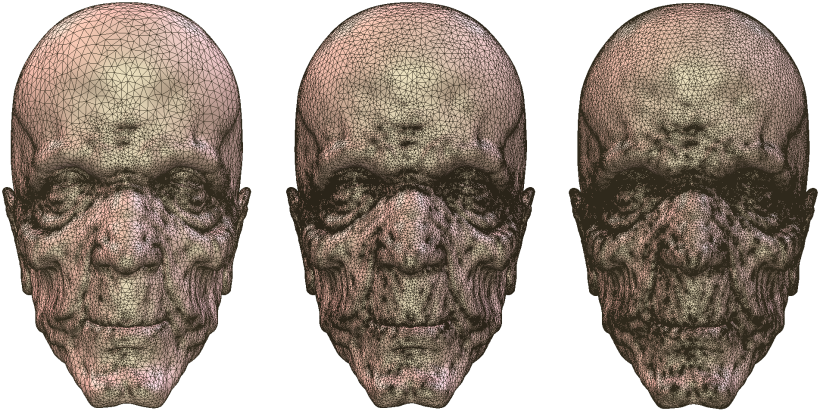

16k 32k 64k

Figure: Multi-resolution Remeshing results.

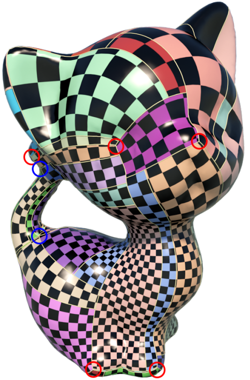

(a) Kitten model

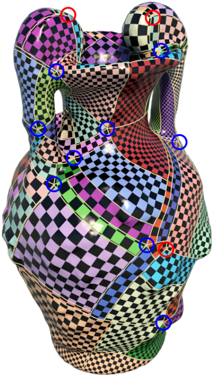

(b) Amphora model

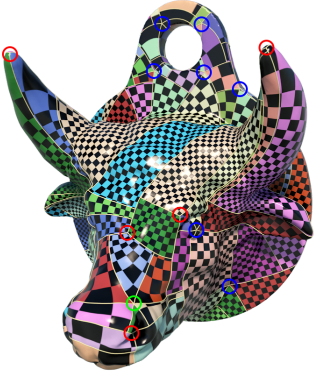

(c) Bull head

Figure: T-Spline conversion.